East European Journal of Physics. **2**. 161–171 (2024)
DOI: 10.26565/2312-4334-2024-2-15 ISSN 2312-4334

THERMAL AND MASS STRATIFICATION EFFECTS ON MHD FLOW PAST AN ACCELERATED VERTICAL PLATE WITH VARIABLE TEMPERATURE AND EXPONENTIAL MASS DIFFUSION EMBEDDED IN A POROUS MEDIUM

Digbash Sahu*, **Rudra Kanta Deka**
Department of Mathematics, Gauhati University, Guwahati, 781014, Assam, India
**Corresponding Author e-mail: digbashsahu79@gmail.com*
Received March 25, 2024; revised April 12, 2024; accepted April 30, 2024

This study looks at how the impacts of thermal and mass stratification on magnetohydrodynamic (MHD) flow alongside a vertically accelerating plate featuring variable temperature and exponential mass diffusion within a porous medium. The Laplace transform technique is utilized to solve the governing equations related to flow, energy, and mass diffusion. Subsequently, the impact of stratification on the flow field, temperature, and mass diffusion is examined. The study indicates that thermal and mass stratification significantly affects the profiles of velocity, temperature, and mass diffusion. Additionally, it has been discovered that a stable state for the velocity is achieved as both stratification parameters are raised, whereas stable states for the temperature and concentration occur when mass stratification is heightened but thermal stratification is reduced.

Keywords: *MHD flow; Thermal stratification; Mass Stratification; Porous Medium; Accelerated Vertical Plate; Variable Temperature; Laplace Transform*

PACS: 47.55.P-, 44.25.+f, 44.05.+e, 47.11.-j

1. INTRODUCTION

The investigation of heat transfer holds importance across various engineering fields, such as in the cooling of electronic devices, nuclear reactors, and gas turbines. Similarly, a grasp of mass transfer is crucial for several chemical engineering applications, like separation processes, distillation, and absorption. This study aims to explore the combined effects of thermal and mass stratification on the behavior of MHD unsteady flow along an accelerated vertical plate, considering variations in mass diffusion and a variable temperature. The influence of thermal and mass stratifications on the behavior of MHD unsteady flows in fluids is significant, and this research seeks to analyze the interaction of these stratifications.

Early work by [1] and [2] laid the groundwork for understanding transient free convection from vertical flat plates. [3] extended this by investigating unsteady natural convection near doubly infinite vertical plates. Later studies explored diverse aspects of this phenomenon. [4] and [5, 6] investigated transient buoyant flows in stratified fluids, while [7] explored convectively driven flows in stably stratified fluids. Porous media were explored in greater detail. [8] investigated unsteady free convection in a fluid-saturated porous medium, and [9] considered heat and mass diffusion flow by natural convection in a porous medium. The influence of radiation and magnetic fields was also examined. The surveyed literature investigates various aspects of magnetohydrodynamic (MHD) and porous medium flow. [10] analyzed MHD boundary layer flow along vertical plates with ramped temperature. [11] study heat sources in MHD flow past an accelerated plate with variable temperature and mass diffusion. [12] explore thermal diffusion in unsteady MHD convective flow. [13, 14, 15, 16] and [17] examine effects like Hall and ion slip, elastico-viscous fluid behavior, and nanofluid flow dynamics in different MHD contexts, emphasizing the influence of porous mediums and thermal conditions on flow properties and heat transfer. More recent research has delved into the effects of chemical reactions in these flows. [18] and [19, 20] studied unsteady flow past vertical plates with chemical reactions in the presence of thermal stratification. Lastly, [21] extended this to porous media, considering mass diffusion, showcasing the breadth and depth of research in this field.

In this study, we present novel contributions by deriving the exact solution through the Laplace transform technique, achieving this with perfect accuracy, which proves to be an extremely effective strategy for obtaining precise solutions. Prior to this work, there has been no exploration of the combined influences of thermal and mass stratification on the behavior of MHD unsteady flow past a vertically accelerating plate embedded within a porous medium, where both temperature and mass diffusion vary. The aim was to analytically explore the dynamics of MHD unsteady flow past such a plate, taking into account the effects of thermal and mass stratification. Subsequently, we compare the results concerning fluid stratification in both thermal and mass

Cite as: D. Sahu, R.K. Deka, East Eur. J. Phys. 2, 161 (2024), https://doi.org/10.26565/2312-4334-2024-2-15

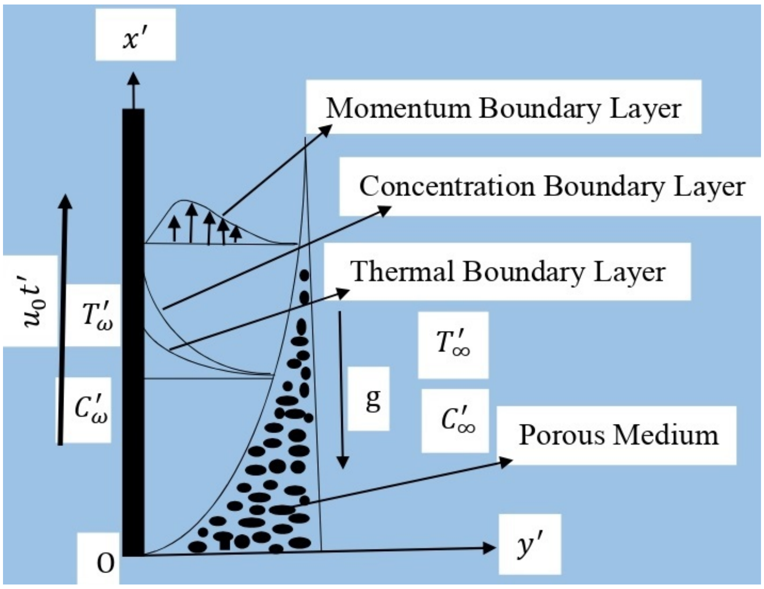

Figure 1. Physical Model and coordinate system

aspects with those of the specific instance lacking any stratification. This study explores and presents the effects of various physical parameters, including γ, ξ, Gr, Gc, the Darcy number (Da), and the Magnetic parameter (M), on the observed profiles through graphical representations. The insights gained from this research hold potential applications across a wide range of industries. For example, the outcomes can be leveraged to enhance thermal system efficiency by minimizing the temperature discrepancy between the walls and the fluid, as well as by accelerating the rate of mass diffusion.

2. MATHEMATICAL ANALYSIS

The governing equations describing the convective movement of an electrically conducting, incompressible, and viscous fluid through a porous medium in presence of a magnetic field, where both mass diffusivity and thermal diffusivity are constant, and incorporating the diffusion-thermo effect, are formulated in vector form as follows:

Momentum Equation

$$\rho\left[\frac{\partial\vec{q}}{\partial t'}+(\vec{q}.\vec{\nabla})\vec{q}\right]=-\vec{\nabla}p+\vec{J}\times\vec{B}+p\vec{g}+\mu\nabla^2\vec{q}-\frac{\mu\vec{q}}{k} \tag{1}$$

Energy Equation

$$\rho C_p\left[\frac{\partial T'}{\partial t'}+(\vec{q}.\vec{\nabla})T'\right]=\alpha\nabla^2T' \tag{2}$$

Concentration Equation

$$\frac{\partial C'}{\partial t'}+(\vec{q}.\vec{\nabla})C'=D\nabla^2C' \tag{3}$$

Consider the MHD unsteady flow of a viscous, incompressible, and stratified fluid over an accelerating vertical plate within a porous medium. The analysis adopts a rectangular Cartesian coordinate system (x', y', t'), where the y' axis is perpendicular to the plate and the x' axis extends vertically upward along the plate. The fluid velocity at any point (x', y', t') is given by $q = (u', 0)$. Initially, at $t' = 0$, the temperature and concentration at the plate are T'_∞ and C'_∞, respectively. For $t' > 0$, the plate accelerates within its own plane at a velocity of u_0t' relative to the gravitational force. Additionally, for $t' > 0$, the temperature drops to $T'_\infty + (T'_w - T'_\infty)At'$, while the concentration increases linearly over time t. Given the plate's infinite dimensions, all flow variables are independent of x', varying only with y' and t'. Thus, under the standard Boussinesq approximation, specific equations are employed to describe the MHD unsteady flow dynamics. The conversion procedure for equations (1)-(3) has already been addressed by Sarma et al. [22]. Consequently, we obtain the following form.

$$\frac{\partial u'}{\partial t'} = g\beta(T'-T'_\infty)+g\beta^*(C'-C'_\infty)+\nu\frac{\partial^2u'}{\partial y'^2}-\frac{\sigma B_0^2u'}{\rho}-\frac{\nu}{k}u' \tag{4}$$

$$\frac{\partial T'}{\partial t'} = \alpha\frac{\partial^2T'}{\partial y'^2}-\gamma'u' \tag{5}$$

$$\frac{\partial C'}{\partial t'} = D\frac{\partial^2 C'}{\partial y'^2} - \xi' u' \tag{6}$$

with the following initial and boundary Conditions:

$$\begin{array}{llll} u' = 0 & T' = T'_\infty & C' = C'_\infty & \forall y', t' \leq 0 \\ u' = u_0 t' & T' = T'_\infty + (T'_w - T'_\infty)At' & C' = C'_\infty + (C'_w - C'_\infty)e^{a't'} & \text{at } y' = 0, t' > 0 \\ u' = 0 & T' \to T'_\infty & C' \to C'_\infty & \text{as } y' \to \infty, t' > 0 \end{array}$$

where a', α, η, ν, D, and Da are respectively constant, thermal diffusivity, similarity parameter, kinematic viscosity, mass diffusion coefficient, darcy number. The "thermal stratification parameter" and "mass stratification parameter" are termed as $\gamma' = \frac{dT'_\infty}{dx'} + \frac{g}{C_p}$ and $\xi' = \frac{dC'_\infty}{dx'}$ respectively. The term "thermal stratification" refers to the combination of vertical temperature advection $\left(\frac{dT'_\infty}{dx'}\right)$, where the temperature of the surrounding fluid is height-dependent, and work of compression $\left(\frac{g}{C_p}\right)$, the rate at which particles in a fluid do reversible work due to compression. And we provide non-dimensional quantities in the following:

$$U = \frac{u'}{(u_0\nu)^{1/3}}, \quad t = t'\left(\frac{u_0^2}{\nu}\right)^{1/3}, \quad y = y'\left(\frac{u_0}{\nu^2}\right)^{1/3}, \quad \theta = \frac{T' - T'_\infty}{T'_w - T'_\infty}, \quad C = \frac{C' - C'_\infty}{C'_w - C'_\infty},$$

$$Gr = \frac{g\beta(T'_w - T'_\infty)}{u_0}, \quad Gc = \frac{g\beta^*(C'_w - C'_\infty)}{u_0}, \quad Pr = \frac{\nu}{\alpha}, \quad Sc = \frac{\nu}{D}, \quad a = a'\left(\frac{\nu}{u_0^2}\right)^{1/3},$$

$$M = \frac{\sigma B_0^2 \nu^{\frac{1}{3}}}{\rho u_0^{\frac{2}{3}}}, \quad Da = k'\left(\frac{u_0^2}{\nu^4}\right)^{1/3}, \quad \gamma = \frac{\gamma' \nu^{2/3}}{u_0^{1/3}(T'_w - T'_\infty)}, \quad \xi = \frac{\xi' \nu^{2/3}}{u_0^{1/3}(C'_w - C'_\infty)}$$

$A = \left(\frac{u_0^2}{\nu}\right)^{1/3}$ is the constant.

$$\frac{\partial U}{\partial t} = Gr\theta + GcC + \frac{\partial^2 U}{\partial y^2} - \left(M + \frac{1}{Da}\right)U \tag{7}$$

$$\frac{\partial \theta}{\partial t} = \frac{1}{Pr}\frac{\partial^2 \theta}{\partial y^2} - \gamma U \tag{8}$$

$$\frac{\partial C}{\partial t} = \frac{1}{Sc}\frac{\partial^2 C}{\partial y^2} - \xi U \tag{9}$$

Non-dimensional forms of initial and boundary Conditions are:

$$\begin{array}{llll} U = 0 & \theta = 0 & C = 0 & \forall y, t \leq 0 \\ U = t & \theta = t & C = e^{at} & \text{at } y = 0, t > 0 \\ U = 0 & \theta \to 0 & C \to 0 & \text{as } y \to \infty, t > 0 \end{array} \tag{10}$$

3. METHOD OF SOLUTION

We discovered that the Laplace transform method produces an equation of non-tractable form for any arbitrary Prandtl or Schmidt number. The non-dimensional governing equations (7)-(9) with boundary conditions (10), are solved for the tractable situation of $Pr = 1, Sc = 1$. Hence, the expressions for velocity, temperature, and concentration profiles can be determined with the help of [23] and [24] are as follows

$$U = \frac{F - Gr}{F - Q}\{g_1(F)\} - \frac{Gc}{F - Q}\{g_2(F) - g_2(Q)\} + \frac{Gr - Q}{F - Q}\{g_1(Q)\} \tag{11}$$

$$\begin{aligned} \theta = & \left(t - \frac{t\gamma Gr}{FQ}\right)\left[(1 + 2\eta^2)erfc(\eta) - \frac{2\eta}{\sqrt{\pi}}e^{-\eta^2}\right] - \frac{\gamma Gce^{at}}{2FQ}\left[e^{-2\eta\sqrt{at}}erfc\left(\eta - \sqrt{at}\right) + e^{2\eta\sqrt{at}}erfc\left(\eta + \sqrt{at}\right)\right] \\ & + \frac{F - Gr}{F - Q}\left\{\frac{\gamma}{F}g_1(F)\right\} + \frac{Gr - Q}{F - Q}\left\{\frac{\gamma}{Q}g_1(Q)\right\} - \frac{\gamma Gc}{F - Q}\left\{\frac{1}{F}g_2(Q) - \frac{1}{Q}g_2(F)\right\} \end{aligned} \tag{12}$$

$$\begin{aligned}
C \;=\; & \frac{t\xi\left\{2FQ - Gr(F-Q)\right\}}{FQ(F-Q)}\left[(1+2\eta^2)erfc(\eta) - \frac{2\eta}{\sqrt{\pi}}e^{-\eta^2}\right] - \frac{(FQ-\xi Gc)e^{at}}{2FQ} \\
& \left[e^{-2\eta\sqrt{at}}erfc\left(\eta-\sqrt{at}\right) + e^{2\eta\sqrt{at}}erfc\left(\eta+\sqrt{at}\right)\right] \\
& +\frac{\xi(F-Gr)}{F-Q}\left\{\frac{1}{F}g_1(F) - \frac{1}{Q}g_1(Q)\right\} - \frac{\xi Gc}{F-Q}\left\{\frac{1}{F}g_2(F) - \frac{1}{Q}g_2(Q)\right\} - \frac{\xi}{Q}\left\{g_1(Q)\right\} \qquad (13)
\end{aligned}$$

Where,

$$\eta = \frac{y}{2\sqrt{t}}, \quad F+Q = M + \frac{1}{Da}, \quad F-Q = \sqrt{\left(M+\frac{1}{Da}\right)^2 - 4(\gamma Gr + \xi Gc)}$$

Also, f_i's are inverse Laplace's transforms given by

$$g_1(p) = L^{-1}\left\{\frac{e^{-y\sqrt{s+p}}}{s^2}\right\}, \quad g_2(p) = L^{-1}\left\{\frac{e^{-y\sqrt{s+p}}}{s-a}\right\}$$

We separate the complex arguments of the error function contained in the previous expressions into real and imaginary parts using the formulas provided by [23].

4. CLASSICAL CASE $(\gamma = 0, \xi = 0)$

We derived solutions for the classical case of no thermal and mass stratification $(\gamma = 0, \xi = 0)$. We want to compare the results of the fluid with thermal and mass stratification to the case with no stratification. Hence, the solutions for the classical case with boundary conditions (10) by using the Laplace transformation are as follows:

$$\theta_c = t\left\{\left(1+2\eta^2\right)erfc(\eta) - \frac{2\eta}{\sqrt{\pi}}e^{-\eta^2}\right\} \qquad (14)$$

$$C_c = \frac{e^{at}}{2}\left[e^{-2\eta\sqrt{at}}erfc\left(\eta-\sqrt{at}\right) + e^{2\eta\sqrt{at}}erfc\left(\eta+\sqrt{at}\right)\right] \qquad (15)$$

$$\begin{aligned}
U_c \;=\; & \left(1-\frac{Gr}{F+Q}\right)g_1(F+Q) - \frac{Gc}{(F+Q)}g_2(F+Q) + \frac{Gc\; e^{at}}{2(F+Q)}\left\{e^{-2\eta\sqrt{at}}erfc\left(\eta-\sqrt{at}\right)\right. \\
& \left. +e^{2\eta\sqrt{at}}erfc\left(\eta+\sqrt{at}\right)\right\} + \frac{tGr}{(F+Q)}\left\{\left(1+2\eta^2\right)erfc(\eta) - \frac{2\eta}{\sqrt{\pi}}e^{-\eta^2}\right\} \qquad (16)
\end{aligned}$$

4.1. Skin-Friction

The non-dimensional Skin-Friction, which is determined as shear stress on the surface, is obtained by

$$\tau = -\left.\frac{dU}{dy}\right|_{y=0}$$

The solution for the Skin-Friction is calculated from the solution of Velocity profile U, represented by (11), as follows:

$$\begin{aligned}
\tau \;=\; & \frac{F-Gr}{F-Q}\left[t\sqrt{F}\; erf(\sqrt{Ft}) + e^{-Ft}\sqrt{\frac{t}{\pi}} + \frac{erf(\sqrt{Ft})}{2\sqrt{F}}\right] - \frac{Gr-Q}{F-Q}\left[t\sqrt{Q}\; erf(\sqrt{Qt}) + e^{-Qt}\sqrt{\frac{t}{\pi}} + \frac{erf(\sqrt{Qt})}{2\sqrt{Q}}\right] \\
& -\frac{Gc}{F-Q}\left[e^{at}\left\{\sqrt{a+F}\; erf(\sqrt{(a+F)t}) - \sqrt{a+Q}\; erf(\sqrt{(a+Q)t})\right\} + \frac{e^{-Ft}-e^{-Qt}}{\sqrt{\pi t}}\right]
\end{aligned}$$

The solution for the Skin-Friction for the classical case is given from the expression (16), which is represented by

$$\begin{aligned}
\tau_c \;=\; & \left(1-\frac{Gr}{F+Q}\right)\left[t\sqrt{F+Q}\; erf(\sqrt{(F+Q)t}) + \sqrt{\frac{t}{\pi}}e^{-(F+Q)t} + \frac{erf(\sqrt{(F+Q)t})}{2\sqrt{(F+Q)t}}\right] + \frac{2Gr}{F+Q}\sqrt{\frac{t}{\pi}} + \\
& \frac{Gc\; e^{at}}{(F+Q)}\sqrt{a}\; erf(\sqrt{at}) + \frac{Gc}{(F+Q)\sqrt{\pi t}} - \frac{Gc\; e^{at}}{(F+Q)}\sqrt{a+(F+Q)}\; erf(\sqrt{(a+F+Q)t}) - \frac{Gc\; e^{(F+Q)t}}{(F+Q)\sqrt{\pi t}}
\end{aligned}$$

4.2. Nusselt Number

The non-dimensional Nusselt number, which is determined as the rate of heat transfer, is obtained by

$$Nu = -\left.\frac{d\theta}{dy}\right|_{y=0}$$

The solution for the Nusselt number is calculated from the solution of Temperature profile θ, represented by (12), as follows:

$$\begin{aligned} Nu \;=\;& 2\sqrt{\frac{t}{\pi}}\left(1-\frac{\gamma Gr}{FQ}\right)-\frac{\gamma Gc}{FQ}\left[e^{at}\sqrt{a}\;erf(\sqrt{at})+\frac{1}{\sqrt{\pi t}}\right]-\frac{\gamma Gc}{F(F-Q)}\left[e^{at}\sqrt{a+F}\;erf(\sqrt{(a+F)t})+\frac{e^{-Ft}}{\sqrt{\pi t}}\right]\\ &+\frac{\gamma(F-Gr)}{F(F-Q)}\left[t\sqrt{F}erf(\sqrt{Ft})+\sqrt{\frac{t}{\pi}}e^{-Ft}+\frac{erf(\sqrt{Ft})}{2\sqrt{F}}\right]+\frac{\gamma Gc}{Q(F-Q)}\\ &\left[e^{at}\sqrt{a+Q}\;erf(\sqrt{(a+Q)t})+\frac{e^{-Qt}}{\sqrt{\pi t}}\right]+\frac{\gamma(Gr-Q)}{Q(F-Q)}\left[t\sqrt{Q}\;erf(\sqrt{Qt})+\sqrt{\frac{t}{\pi}}\;e^{-Qt}+\frac{erf(\sqrt{Qt})}{2\sqrt{Q}}\right]\end{aligned}$$

The solution for the Nusselt number for the classical case is given from the expression (14), which is represented by

$$Nu_c = 2\sqrt{\frac{t}{\pi}}$$

4.3. Sherwood Number

The non-dimensional Sherwood number, which is determined as the rate of mass transfer, is obtained by

$$Sh = -\left.\frac{dC}{dy}\right|_{y=0}$$

The solution for the Sherwood number is calculated from the solution of Concentration profile C, represented by (13), as follows:

$$\begin{aligned} Sh \;=\;& \left(1+\frac{\xi Gc(Q-F)}{FQ(F-Q)}\right)\left[e^{at}\sqrt{a}\;erf(\sqrt{at})+\frac{1}{\sqrt{\pi t}}\right]-\frac{2\xi(2FQ-Gr(F+Q))}{FQ(F-Q)}\sqrt{\frac{t}{\pi}}-\frac{\xi Gc}{F(F-Q)}\left[e^{at}\sqrt{a+F}\right.\\ &\left.erf(\sqrt{(a+F)t})+\frac{e^{-Ft}}{\sqrt{\pi t}}\right]+\frac{\xi(F-Gr)}{F(F-Q)}\left[t\sqrt{F}\;erf(\sqrt{Ft})+\sqrt{\frac{t}{\pi}}\;e^{-Ft}+\frac{erf(\sqrt{Ft})}{2\sqrt{F}}\right]+\frac{\xi Gc}{Q(F-Q)}\\ &\left[e^{at}\;\sqrt{a+Q}\;erf(\sqrt{(a+Q)t})+\frac{e^{-Qt}}{\sqrt{\pi t}}\right]+\frac{\xi(Gr-Q)}{Q(F-Q))}\left[t\sqrt{Q}\;erf(\sqrt{Qt})+\sqrt{\frac{t}{\pi}}\;e^{-Qt}+\frac{erf(\sqrt{Qt})}{2\sqrt{Q}}\right]\end{aligned}$$

The solution for the Sherwood number for the classical case is given from the expression (15), which is represented by

$$Sh_c = e^{at}\sqrt{a}\;erf(\sqrt{at})+\frac{1}{\sqrt{\pi t}}$$

5. RESULT AND DISCUSSIONS

We computed numerical values of velocity, temperature, concentration, skin friction, Nusselt number, and Sherwood number from their solutions derived in the preceding sections, for various values of the physical parameters γ, ξ, Gr, Gc, M and Da. This allowed us to get a better understanding of the physical significance of the problem. Moreover, using MATLAB, we plotted them in Figures 2-22.

Figure 2 illustrates the impact of thermal and mass stratification on velocity profiles, showing that both types of stratification lead to reduced velocities. When one form of stratification is held constant, an increase in the other type further decreases velocity. In the same way that [7] shows that fluid velocity drops for thermal stratification $\gamma > 0$, we find that this is also the case for mass stratification $\xi > 0$. Enhancing the parameter of thermal stratification (γ) diminishes the convective potential across the hot plate and the adjacent fluid, reducing the buoyancy force and, subsequently, the flow velocity. Similarly, an increase in the mass stratification (ξ) value leads to a lower concentration gradient between the surface and its environment, diminishing the buoyancy's upward force and thus slowing down the fluid flow. Therefore, the presence of both thermal and mass stratification results in a reduced fluid velocity compared to conditions without stratification.

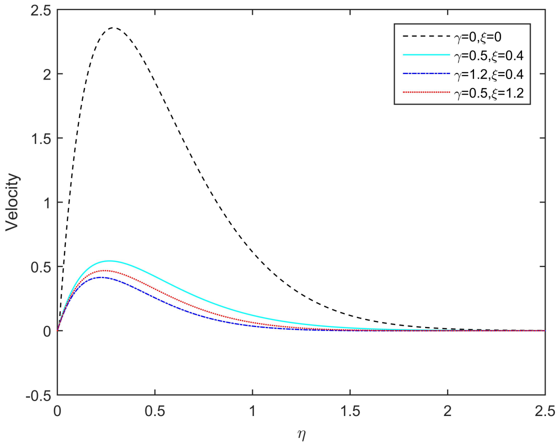

Figure 2. Effects of γ and ξ on Velocity Profile for $Gr = 5, Gc = 5, M = 2, Da = 0.5, t = 1.5, a = 0.2,$

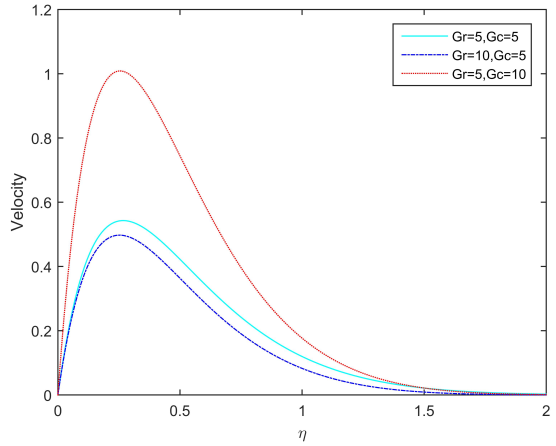

Figure 3. Effects of Gr and Gc on Velocity Profile for $\gamma = 0.5, \xi = 0.4, M = 2, Da = 0.5, t = 1.5, a = 0.2$

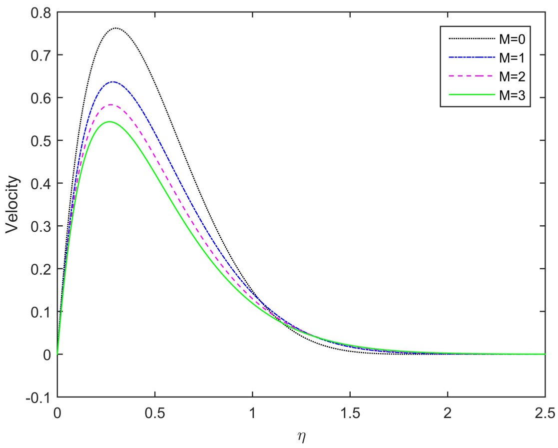

Figure 4. Effects of M on Velocity Profile for $Gr = 5, Gc = 5, \gamma = 0.5, \xi = 0.4, Da = 0.5, t = 1.5, a = 0.2,$

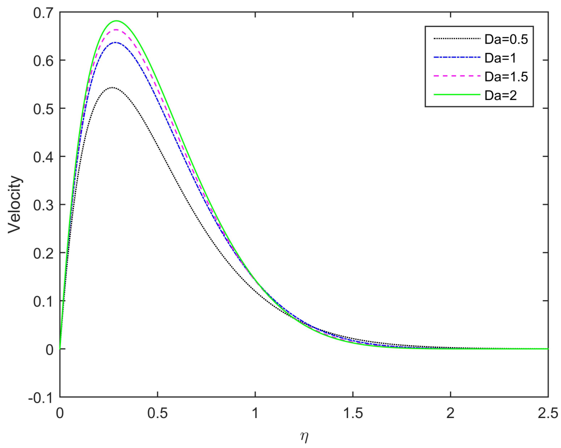

Figure 5. Effects of Da on Velocity Profile for $Gr = 5, Gc = 5, \gamma = 0.5, \xi = 0.4, M = 2, t = 1.5, a = 0.2,$

Hence, both thermal and mass stratification play a crucial role in establishing a stable stratified flow. As seen in Figure 3, Raising the value of Gc leads to a higher velocity, while a rise in Gr causes a decrease in velocity. We can observe from Figure 4 that velocity decreases as (M) grows. Figure 5 shows that as Da and the fluid's porosity increase, there is an elevation in the velocity profile, enabling the fluid particles to move more smoothly.

Figure 6 demonstrates the impact of thermal and mass stratification on the temperature profile. While mass stratification leads to an increase in temperature, an increase in thermal stratification is associated with a reduction in temperature. An increase in thermal stratification (γ) causes the temperature gradient between the vertical plate and the adjacent fluid to diminish. Consequently, this results in a thicker thermal boundary layer and a lower temperature. As shown in Figures 7, and 9, the temperature drops as $Gr, Gc,$ and Da increase and in Figure 8 the temperature increases as M increase. In Figure 10, fluid concentration decreases with increasing mass stratification parameters but increases with increasing thermal stratification. As shown in Figures 11, 12, and 13 the effects of $Gr, Gc, Da,$ and M on concentration are identical to those seen for temperature profiles.

Figures 14, 15, and 16 plot the two stratification's effects on fluid velocity, temperature, and concentration over time. The velocity grows infinitely with time for the Classical case but reaches a steady state when both stratifications are present. The presence of both stratifications influences the temperature profile over time, but an increase in thermal stratification has a more pronounced effect in slowing down the temperature increase compared to an increase in mass stratification. The concentration increases over time, highest with no stratification, and less as thermal or mass stratification values rise.

In Figure 17, skin friction decreases with time in the presence of both stratification compared to no stratification. It decreases over time, with the lowest values occurring for the highest Gc at a constant Gr, as shown in Figure 18. Figures 19, 20, 21and 22 for both nusselt and sherwood numbers, values rise with time.

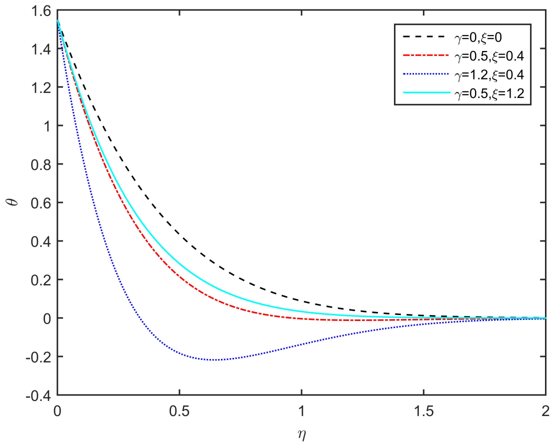

Figure 6. Effects of γ and ξ on Temperature Profile for $Gr = 5, Gc = 5, M = 2, Da = 0.5, t = 1.5, a = 0.2$

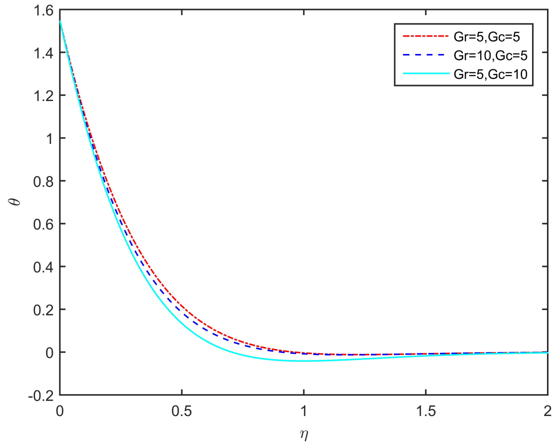

Figure 7. Effects of Gr and Gc on Temperature Profile for $\gamma = 0.5, \xi = 0.4, t = 1.5, M = 2, Da = 0.5, a = 0.2$

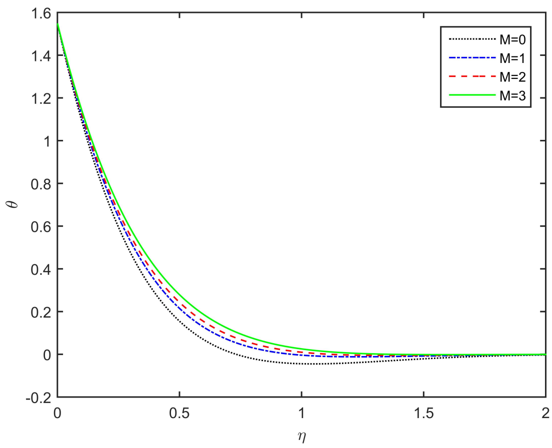

Figure 8. Effects of M on Temperature Profile for $Gr = 5, Gc = 5, \gamma = 0.5, \xi = 0.4, t = 1.5, Da = 0.5, a = 0.2$

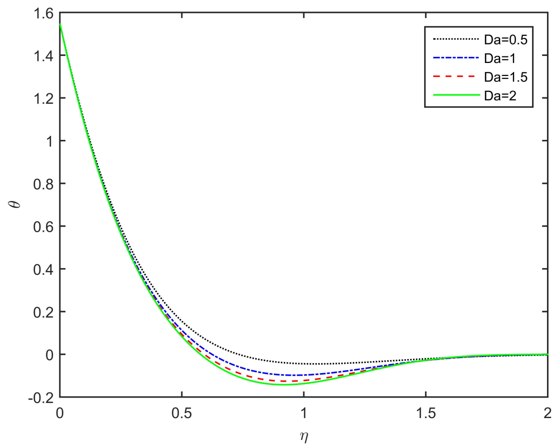

Figure 9. Effects of Da on Temperature Profile for $Gr = 5, Gc = 5, \gamma = 0.5, \xi = 0.4, t = 1.5, M = 2, a = 0.2$

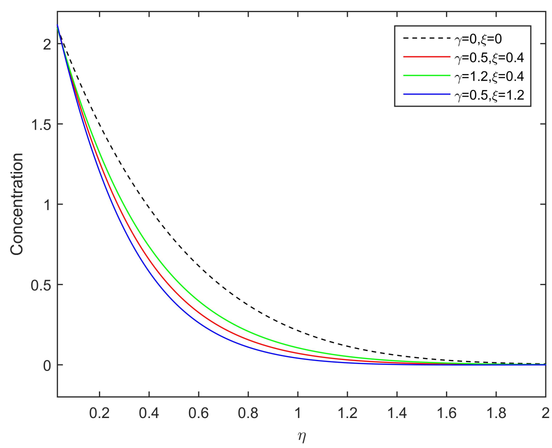

Figure 10. Effects of γ and ξ on Concentration Profile for $Gr = 5, Gc = 5, Da = 0.5, t = 1, M = 2, a = 0.2$

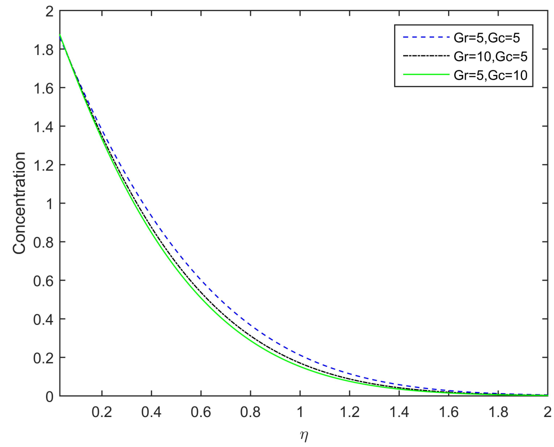

Figure 11. Effects of Gr and Gc on Concentration Profile for $\gamma = 0.5, \xi = 0.4, t = 0.5, M = 2, Da = 0.5, a = 0.2$

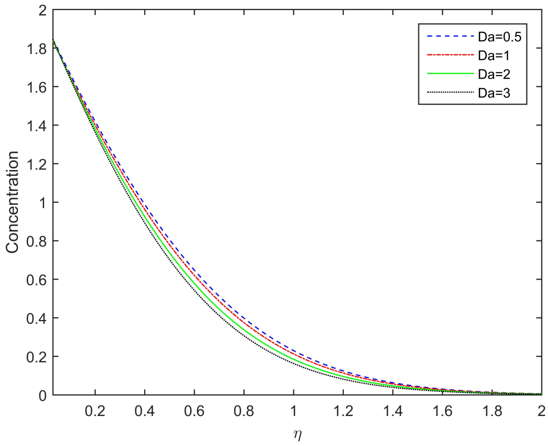

Figure 12. Effects of Da on Concentration Profile for $Gr = 5, Gc = 5, \gamma = 0.5, \xi = 0.4, t = 0.5, M = 2, a = 0.2$

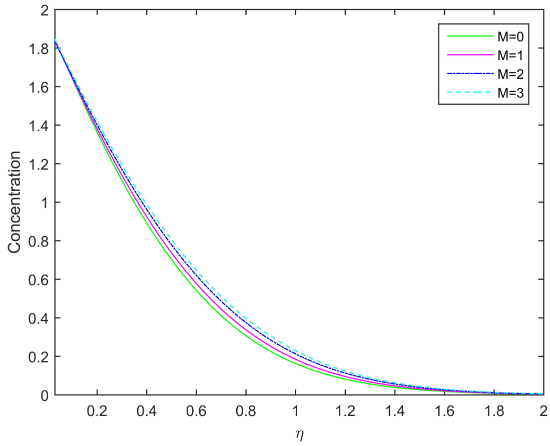

Figure 13. Effects of M on Concentration Profile for $Gr = 5, Gc = 5, \gamma = 0.5, \xi = 0.4, t = 0.5, Da = 0.5, a = 0.2$

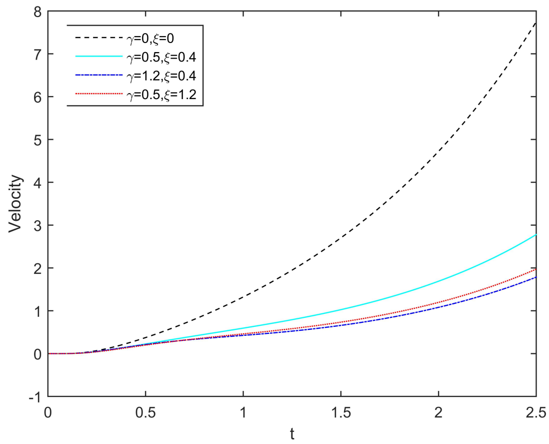

Figure 14. Effects of γ and ξ on Velocity Profile against time for $Gr = 5, Gc = 5, M = 2, Da = 0.5, a = 0.2, y = 1.4$

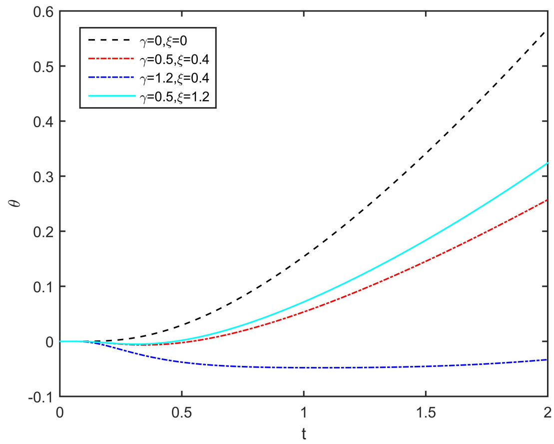

Figure 15. Effects of γ and ξ on Temperature Profile against time for $Gr = 5, Gc = 5, M = 2, Da = 0.5, a = 0.2, y = 1.4$

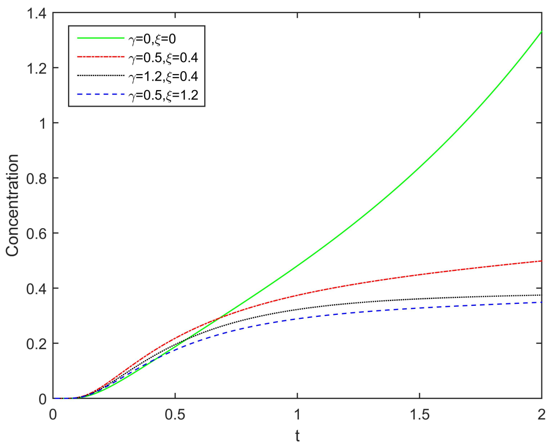

Figure 16. Effects of γ and ξ on Concentration Profile against time for $Gr = 5, Gc = 5, M = 2, Da = 0.5, a = 0.2, y = 1.4$

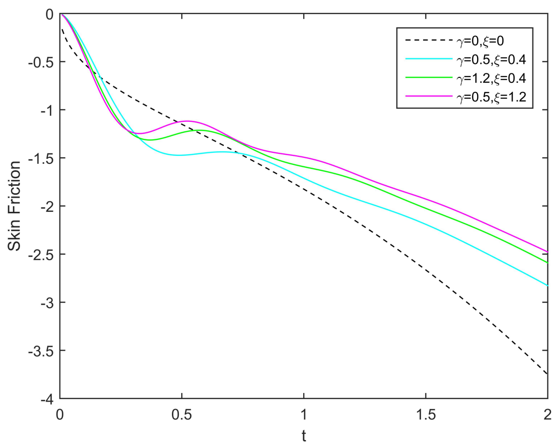

Figure 17. Effects of γ and ξ on Skin friction for $Gr = 5, Gc = 5, M = 2, Da = 0.5, a = 0.2$

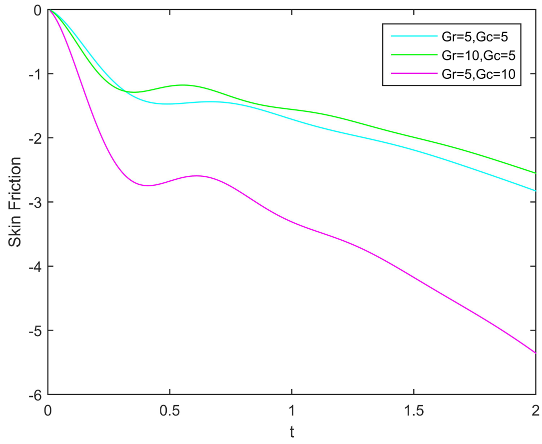

Figure 18. Effects of Gr and Gc on Skin friction for $\gamma = 0.5, \xi = 0.4, M = 2, Da = 0.5, a = 0.2$

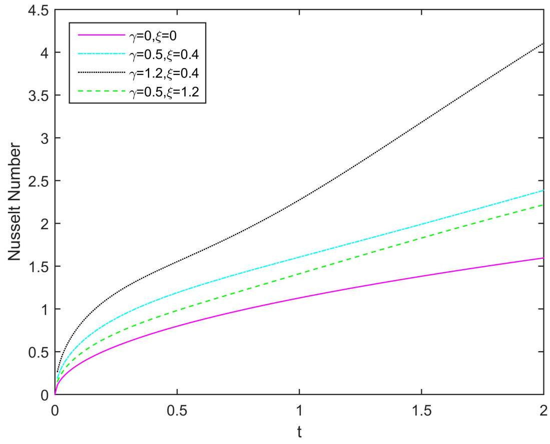

Figure 19. Effects of γ and ξ on Nusselt Number for $Gr = 5, Gc = 5, M = 2, Da = 0.5, a = 0.2$

Higher thermal stratification dampens the increase for nusselt and more so for sherwood, while varying mass stratification shows mixed effects. Higher Gr boosts sherwood's growth at a constant Gc.

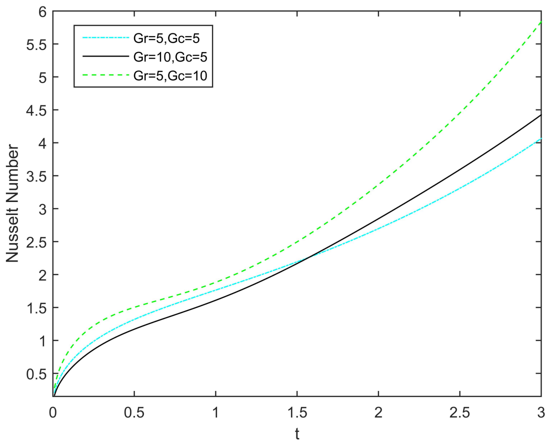

Figure 20. Effects of Gr and Gc on Nusselt Number for $\gamma = 0.5, \xi = 0.4, M = 2, Da = 0.5, a = 0.2$

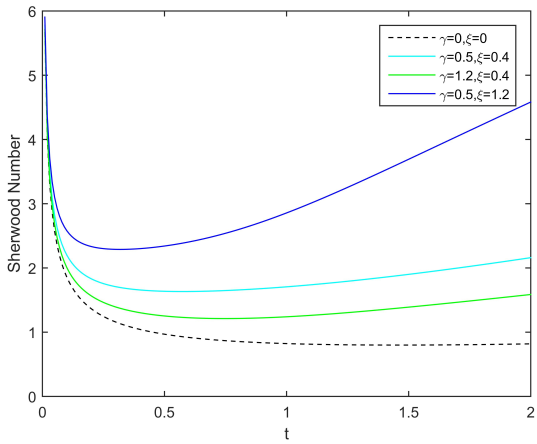

Figure 21. Effects of γ and ξ on Sherwood Number for $Gr = 5, Gc = 5, M = 2, Da = 0.5, a = 0.2$

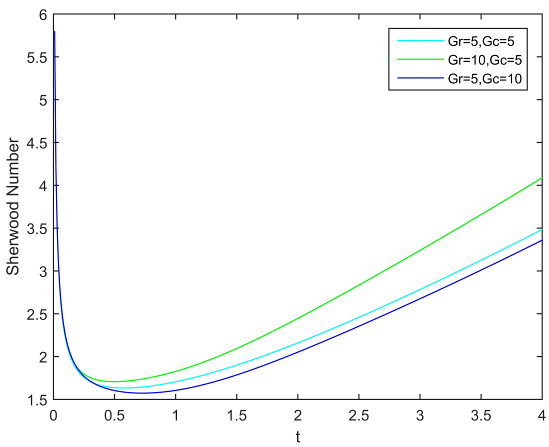

Figure 22. Effects of Gr and Gc on Sherwood Number for $\gamma = 0.5, \xi = 0.4, M = 2, Da = 0.5, a = 0.2$

6. CONCLUSION

The findings from this research indicate that thermal and mass stratification notably diminishes velocity over time, leading the system to achieve equilibrium. For conditions of increased mass stratification and decreased thermal stratification, the system's temperature and concentration levels stabilize. With the concurrent presence of both types of stratification, there is a gradual decrease in skin friction. Additionally, time enhances heat and mass transfer rates, with higher mass stratification and lower thermal stratification increasing both nusselt and sherwood numbers more markedly. These results hold significant implications for the design of porous media systems tailored to manage MHD unsteady flow with stratification features.

ORCID

Digbash Sahu, https://orcid.org/0009-0005-8925-2048; **Rudra Kanta Deka**, https://orcid.org/0009-0007-1573-4890

REFERENCES

[1] R. Siegel, "Transient free convection from a vertical flat plate," Transactions of the American Society of Mechanical Engineers, **80**(2), 347-357 (1958). https://doi.org/10.1115/1.4012369.

[2] E.R. Menold, and K.T. Yang, "Asymptotic solutions for unsteady laminar free convection on a vertical plate," Trans ASME: J. Appl. Mech. **29**, 124-126 (1962). http://doi:10.1115/1.3636443.

[3] J.A. Schetz, and R. Eichhorn, "Unsteady natural convection in the vicinity of a doubly infinite vertical plate," Trans ASME C: J. Heat Transfer, **84**(4), 334-338 (1962). https://doi.org/10.1115/1.3684386

[4] U.N. Das, R.K. Deka, and V.M. Soundalgekar, "Transient free convection flow past an infinite vertical plate with periodic temperature variation," J. Heat Transfer, **121**(4) 1091-1094 (1999). https://doi.org/10.1115/1.2826063

[5] J.S. Park, and J.M. Hyun, "Technical Note Transient behavior of vertical buoyancy layer in a stratified fluid," International journal of heat and mass transfer, **41**(24), 4393-4397 (1998). https://doi.org/10.1016/S0017-9310(98)00175-6

[6] J.S. Park, "Transient buoyant flows of a stratified fluid in a vertical channel," KSME international journal, **15**, 656-664 (2001). http://doi:10.1007/bf03184382

[7] A. Shapiro, and E. Fedorovich, "Unsteady convectively driven flow along a vertical plate immersed in a stably stratified fluid," Journal of Fluid Mechanics, **498**, 333-352 (2004). https://doi.org/10.1017/S0022112003006803

[8] E. Magyari, I. Pop, and B. Keller, "Unsteady free convection along an infinite vertical flat plate embedded in a stably stratified fluid-saturated porous medium," Transport in porous media, **62**, 233-249 (2006). https://DOI10.1007/s11242-005-1292-6

[9] R.C. Chaudhary, and A. Jain, "MHD heat and mass diffusion flow by natural convection past a surface embedded in a porous medium," Theoretical and Applied Mechanics, **36**(1), 1-27 (2009). https://doi.org/10.2298/TAM0901001C

[10] Y.D. Reddy, B.S. Goud, and M.A. Kumar, "Radiation and heat absorption effects on an unsteady MHD boundary layer flow along an accelerated infinite vertical plate with ramped plate temperature in the existence of slip condition," Partial Differential Equations in Applied Mathematics, **4**, 100166 (2021). https://doi.org/10.1016/j.padiff.2021.100166

[11] A. Selvaraj, and E. Jothi, "Heat source impact on MHD and radiation absorption fluid flow past an exponentially accelerated vertical plate with exponentially variable temperature and mass diffusion through a porous medium," Materials Today: Proceedings, **46**, 3490-3494 (2021). https://doi.org/10.1016/j.matpr.2020.11.919

[12] S. Sarma, and A. Nazibuddin, "Thermal diffusion effect on unsteady MHD free convective flow past a semi-infinite exponentially accelerated vertical plate in a porous medium," Canadian Journal of Physics, **100**(10), 437-451 (2022). https://doi.org/10.1139/cjp-2021-0361

[13] M.V. Krishna, and A.J. Chamkha, "Hall and ion slip effects on MHD rotating flow of elastico-viscous fluid through porous medium," International Communications in Heat and Mass Transfer, **113**, 104494 (2020). https://doi.org/10.1016/j.icheatmasstransfer.2020.104494

[14] M.V. Krishna, K. Jyothi, and A.J. Chamkha, "Heat and mass transfer on MHD flow of second-grade fluid through porous medium over a semi-infinite vertical stretching sheet," Journal of Porous media, **23**(8), (2020). https://doi.org/10.1615/JPorMedia.2020023817

[15] M.V. Krishna, N.A. Ahamad, and A.J. Chamkha, "Hall and ion slip effects on unsteady MHD free convective rotating flow through a saturated porous medium over an exponential accelerated plate," Alexandria Engineering Journal, **59**(2), 565-577 (2020). https://doi.org/10.1016/j.aej.2020.01.043

[16] M.V. Krishna, and A.J. Chamkha, "Hall and ion slip effects on magnetohydrodynamic convective rotating flow of Jeffreys fluid over an impulsively moving vertical plate embedded in a saturated porous medium with Ramped wall temperature," Numerical Methods for Partial Differential Equations, **37**(3), 2150-2177 (2021). https://doi.org/10.1002/num.22670

[17] M.V. Krishna, and A.J. Chamkha, "Hall and ion slip effects on MHD rotating boundary layer flow of nanofluid past an infinite vertical plate embedded in a porous medium," Results in Physics, **15**, 102652 (2019). https://doi.org/10.1016/j.rinp.2019.102652

[18] N. Kalita, R. K. Deka, R. S. Nath, "Unsteady Flow Past an Accelerated Vertical Plate with Variable Temperature in Presence of Thermal Stratification and Chemical Reaction," East European Journal of Physics, (3), 441-450 (2023). https://doi.org/10.26565/2312-4334-2023-3-49

[19] R. S. Nath, R. K. Deka, "The Effects of Thermal Stratification on Flow Past an Infinite Vertical Plate in Presence of Chemical Reaction," East European Journal of Physics, (3), 223-232 (2023). https://doi.org/10.26565/2312-4334-2023-3-19

[20] R.S. Nath, R.K. Deka, and H. Kumar, "The Effect of Thermal Stratification on Unsteady Parabolic Flow Past An Infinite Vertical Plate With Chemical Reaction," East European Journal of Physics, (4), 77–86 (2023). https://doi.org/10.26565/2312-4334-2023-4-08

[21] H. Kumar, and R.K. Deka, "Thermal and Mass Stratification Effects on Unsteady Flow Past an Accelerated Infinite Vertical Plate with Variable Temperature and Exponential Mass Diffusion in Porous Medium," East European Journal of Physics, (4) 87–97 (2023), https://doi.org/10.26565/2312-4334-2023-4-09

[22] S. Sarma, and N. Ahmed, "Dufour effect on unsteady MHD flow past a vertical plate embedded in porous medium with ramped temperature," Scientific Reports, **12**(1), 13343 (2022). https://doi.org/10.1038/s41598-022-15603-x.

[23] M. Abramowitz, I.A. Stegun, and R.H. Romer, "Handbook of mathematical functions with formulas, graphs, and mathematical tables." American Journal of Physics, **56**(10), 958 (1988). https://doi.org/10.1119/1.15378

[24] R.B. Hetnarski, "An algorithm for generating some inverse Laplace transforms of exponential form," Zeitschrift für angewandte Mathematik und Physik ZAMP, **26**, 249-253 (1975). https://doi.org/10.1007/bf01591514

ВПЛИВ ТЕРМІЧНОЇ ТА МАСОВОЇ СТРАТИФІКАЦІЇ НА МГД-ПОТІК ПОВЗ ПРИСКОРЕНУ ВЕРТИКАЛЬНУ ПЛАСТИНУ ВБУДОВАНУ В ПОРИСТЕ СЕРЕДОВИЩЕ ЗІ ЗМІННОЮ ТЕМПЕРАТУРОЮ ТА ЕКСПОНЕНЦІАЛЬНОЮ МАСОВОЮ ДИФУЗІЄЮ

Дігбаш Саху, **Рудра Канта Дека**

Факультет математики, Університет Гаухаті, Гувахаті, 781014, Ассам, Індія

У цьому дослідженні розглядається вплив термічної та масової стратифікації на магнітогідродинаміку (МГД) поряд із вертикально прискорюваною пластиною зі змінною температурою та експоненціальною масовою дифузією в пористому середовищі. Техніка перетворення Лапласа використовується для вирішення визначальних рівнянь, пов'язаних із дифузією потоку, енергії та маси. Далі досліджується вплив стратифікації на поле течії, температуру та дифузію маси. Дослідження показує, що теплова та масова стратифікація суттєво впливає на профілі швидкості, температури та дифузії маси. Крім того, було виявлено, що стабільний стан для швидкості досягається, коли обидва параметри стратифікації підвищуються, тоді як стабільні стани для температури та концентрації виникають, коли масова стратифікація підвищується, але термічна стратифікація зменшується.

Ключові слова: *МГД потік; термічна стратифікація; масове розшарування; пористе середовище; прискорена вертикальна пластина; змінна температура; перетворення Лапласа*